

Review

# Subsidence Mechanism and Stability Assessment Methods for Partial Extraction Mines for Sustainable Development of Mining Cities—A Review

Yang Yu <sup>1</sup> , Shen-En Chen <sup>2</sup> , Ka-Zhong Deng <sup>1,\*</sup> , Peng Wang <sup>3</sup> and Hong-Dong Fan <sup>1,4</sup>

<sup>1</sup> School of Environment Science and Spatial Information, China University of Mining and Technology, Xuzhou 221116, China; yuyang1989cumt@gmail.com (Y.Y.); cumtfhd@163.com (H.-D.F.)

<sup>2</sup> Department of Civil and Environmental Engineering, University of North Carolina at Charlotte, 9201 University City Blvd., Charlotte, NC 28223, USA; schen12@uncc.edu

<sup>3</sup> School of Mechanics and Civil Engineering, China University of Mining and Technology, Xuzhou 221116, China; pwang@cumt.edu.cn

<sup>4</sup> State Key Laboratory of Geohazard Prevention and Geoenvironment Protection, Chengdu University of Technology, Chengdu 610059, China

\* Correspondence: kzdeng@cumt.edu.cn; Tel.: +86-0516-8388-5986

Received: 14 November 2017; Accepted: 4 January 2018; Published: 6 January 2018

**Abstract:** Partial extraction methods such as underground strip pillar mining or room-and-pillar mining are widely adopted techniques to control ground subsidence. However, pillar failure in partial extraction mines may introduce violent secondary ground collapses. The stability of partial extraction mines dictates the safety of ground surface structures and the environmental health state of the surrounding mining areas. To reuse mining subsidence lands, it is necessary to evaluate the stability of the land through mine subsidence assessments. This paper summarizes current pillar stability assessment methods and their limitations, and the rock mechanics associated with the stability of abandoned mines. The effects of multiple factors that affect mine stability are discussed in detail; special attention has been extended to discuss the weathering effects associated with infused water and spontaneous combustion, as these are some key reasons for pillar strength degradation in abandoned mines. The mechanism of mine collapse and the corresponding post-mining disasters are also summarized. Finally, suggestions and strategies to improve current mine stability assessment methods are proposed based on the perspective of subsidence control.

**Keywords:** coal mine; stability assessment; pillar strength; pillar load; ground subsidence; room-and-pillar mining; underground strip pillar mining

## 1. Introduction

Mining typically results in substantial abandoned mine lands that are problematic and can cause hazards to the environment [1]. Mining-induced land waste is a major environmental problem in a sustainability context [2]. According to the Bureau of Land Management of the U.S., there are currently about 500 thousand abandoned mines in the U.S. and many of them present serious threats to the environment [1]. A similar problem pervades all mineral rich nations, for example, since 2005, China had over 809.6 thousand hectares of area with abandoned mines and 1439 thousand hectares of surface land area were deemed wasted [3]. The subsidence land resulting from underground mining is an important source of abandoned mine lands. Most of the abandoned underground mines are documented in old mine maps, such as in Figure 1, showing massive rooms and pillars.

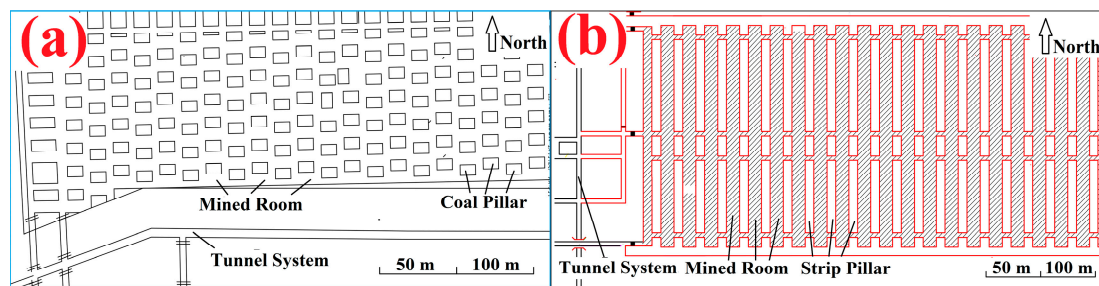


**Figure 1.** Typical abandoned mines of partial extraction from China: (a) room-and-pillar mine; (b) strip pillar mine. Massive coal pillars and voids are left underground.

The partial extraction methods such as underground strip pillar mining (some researchers also used the term “strip mining”, caution should be taken to note that the “strip mining” usually refers to surface mining) or room-and-pillar mining (bord-and-pillar mining) were sometimes adopted to control strata movement and reduce mining subsidence. However, partial extraction methods may result in more severe post-mining hazards if mines collapse in the future. The use of mining-influenced land is restricted because of such uncertainty of ground surface stability. Perhaps the most severe damage brought about by the collapse of abandoned mines is the violent and massive ground collapse in room-and-pillar mines. Several mining areas in China have already begun to be subjected to these violent disasters. For example, from 2004 to 2016, the Yulin mining area was subjected to 96 mining-induced earthquakes with magnitudes exceeding two on the Richter scale [4]. As a result, panic has spread among residents living around mining areas.

Besides the engineering safety, there are also long-term effects on the environment. For example, localized pillar failures may introduce atmospheric air into the abandoned mine shafts and thus increase the possibility of spontaneous combustion of the residual coal. This will further increase the danger of massive cavity collapse, and will also allow greenhouse and toxic gases to return to the atmosphere. According to incomplete statistics, 2.3 billion tons of coal remained as coal pillars near Ordos, China in 2007 [5]. The remnant coal presents a long-term stability issue for future land use and sustainable development. On the other hand, mining subsidence affects the soil physical properties (i.e., soil moisture, hardness, porosity) and chemical properties (nutrients, pH value), which will further affect the soil quality and plant community around the mining areas [6,7]. The degradation of soil quality and plant community structures induced by mine subsidence can last at least 10 years with natural succession [7]. The long-term effectiveness of ecological remediation thus depends on land stability. Finally, the stability of partial extraction mines affects the environment of water resources [8,9]. A stable partial extraction mine can protect the integrity of overburden and preserve a water body, while mine collapse will lead to overburden strata failures, sinkholes or ground fissures, and the water from aquifer or from ground surfaces can leak into the underground voids through the fissures, finally resulting in a decrease in water resources near the ground surface [8,9]. Moreover, the water quality in mining areas may degrade because the fissures can serve as channels to introduce hazardous contaminants from the ground surface and underground voids into the aquifer [9]. Therefore, stability evaluations of mining-influenced land are an important part of land use [10] and the sustainable development of mining cities.

When facing mine subsidence, the key issues of concern are: the stability of the ground surface, the time and extent of collapse, and the associated disasters, the effect on surface structures and effects on terrestrial life. Figure 2 shows a scenario of localized subsidence during room-and-pillar collapse and an idealized subsidence basin. Mining subsidence was studied and utilized to evaluate the hazardous mining influences, in which the mine stability and damage from mining on infrastructure are evaluated by the ground surface displacement [11,12]. For longwall roof-caving mining, such displacement-based mine stability evaluation is reliable, as the ground movements are continuous, and the overburden strata can fully subside in a relative short period. By analyzing the ground surface subsidence laws,

it is easier to know whether a mine has reached a final stabilized state. However, unlike longwall mining, pillar collapses associated with partial extraction mines may result in secondary strata collapse, making it difficult to evaluate mine stability with ground displacement measurements alone. Hence, existing mine stability assessment methods based on classical subsidence theories cannot address the long-term behaviors sufficiently. Therefore, this paper presents a comprehensive review of the mechanics of mine failures (summarized in Figure 3). As the secondary ground subsidence induced by mine collapse is more violent and is harder to predict, special attention was paid to the stability of partial extraction mines (especially room-and-pillar mining). In this paper, current stability assessment methods for partial extraction mines are summarized, and suggestions on ways to improve the stability assessment of abandoned mines are offered.

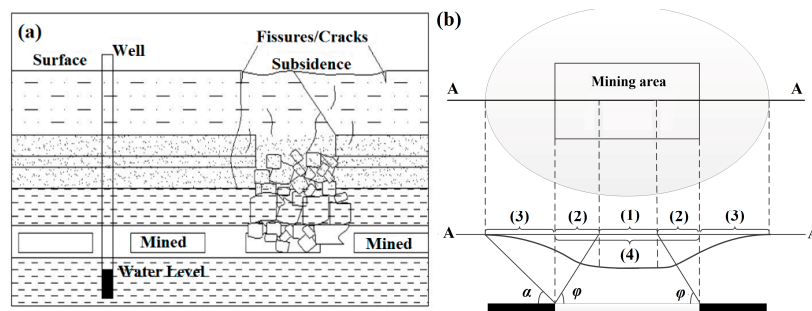


**Figure 2.** Schematic drawings of (a) localized subsidence due to room-and-pillar collapse and (b) continuous mining subsidence:  $\alpha$  stands for boundary angle of subsidence range;  $\phi$  stands for maximum subsidence angle; and area (1) for uniform subsidence; non-uniform compressive area (2) and tensile area (3).

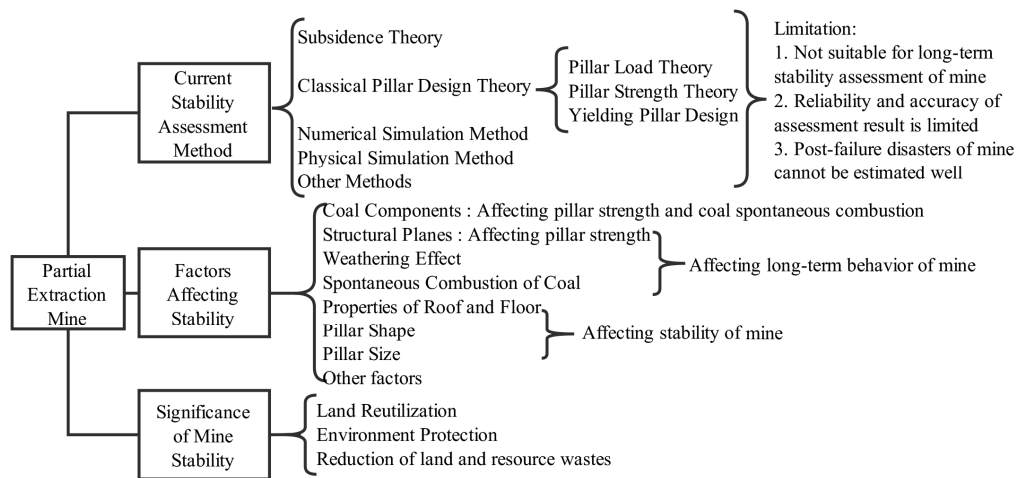


**Figure 3.** Causation-theory relations for partial extraction mine voids stability analysis

## 2. Abandoned Mine Stability Assessment Methods for Partial Extraction

### 2.1. The Classic Methods

Massive coal pillars will be left underground to support the overburden in partial extraction mines, hence, the stability of coal pillars is a critical element controlling mine stability, and the stability assessment of the residual coal pillars can refer to pillar design methods. Mark [13,14] separated classical design methods into empirical safety factor methods and analytical “yielding pillar” methods: The safety factor methods calculate the safety factor by dividing the strength of the coal pillar by the stress applied, and the yielding pillar design methods consider the plastic deformation of the pillars. Classic methods look at the following elements.

### 2.1.1. Pillar Load

The loads applied to coal pillars include the development loads and the abutment loads, and the latter usually appear near the abutment seams [13]. Widely-used load theories include pressure arch (PAT), tributary area (TAT) and beam theories [15–17]. Figure 4 shows the typical conception of different kinds of loads on pillars. In Figure 4,  $P_A$  is the abutment load,  $P_C$  is the load loss due to roof caving or load transfer, and  $P_T$  is the TAT load. The PAT assumes that an arch will form above the coal seam carrying most of the overburden weights, the coal seam near arch springing will carry  $P_A$  and the pillars below the arch will carry  $P_C$ ; while TAT assumes that the overburden load is evenly distributed among the pillars, thus, each pillar will carry  $P_T$  if the rooms are formed (Figure 4a,b), but it may overestimate the stress on the coal pillars [13,18]. At first, the strata properties were not considered in the load calculation, Heasley [19,20], Singh et al. [21] and Rezaei et al. [22] modified the theory and included the mechanical properties of overburden and coal seams, thus improving the accuracy of pillar stress estimation.

Beam theories such as cantilever beam, masonry beam and the Winkler foundation beam, etc. treat the roof and pillars as the combination of different kinds of beams and analyzed the pillar stress based on structural mechanics [17,23]. These methods analyzed the structures of overburden strata and considered the interactions between roof stability and loads on the coal seam, but are not as popular as PAT and TAT in pillar design. However, the beam theories provide an easy way to analyze the roof stability, because the laminated overburden strata can be treated as the combination of different kinds of beam (e.g., Voussoir beam, cantilever beam) [23–25].

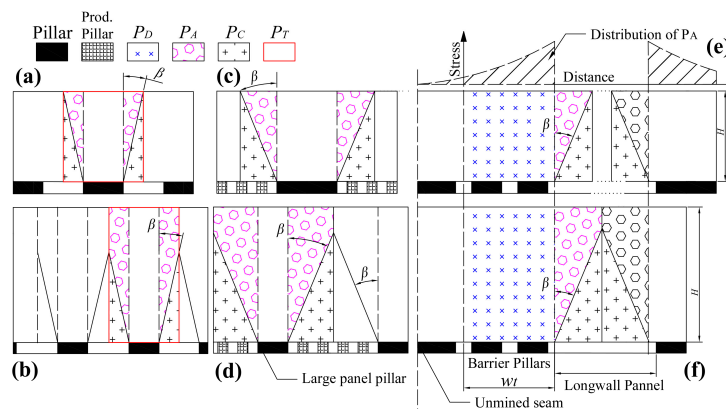


**Figure 4.** The pillar load models: (a–d) are pillar load models in room-and-pillar mining or underground strip pillar mining; (e,f) are pillar load models in longwall mining. (a) is for the pillars with the same size and the mining panel is large; (b) is for the pillars with the same size and the mining panel is small. (c) is for the pillars with different sizes and the mining panel is large; (d) is for the pillars with different sizes and the mining panel is small. In (c,d), the large panel pillars carry more load than small production (Prod.) pillars. The longwall pillar load calculation considered the load distribution in (e,f).  $P_T$  for TAT load;  $P_A$  for abutment load;  $P_C$  for load loss due to roof caving or load transfers to production pillars;  $P_D$  for the development load.

Equation (1), the parameters of which are summarized in Table 1, can be used for 2D (two-dimensional) and 3D (three-dimensional) pillar stress calculation of partial extraction mines:

$$P = \frac{P_T - P_C}{w_p L_p^a} = \gamma H \frac{(w_p + w_c)(L_p + w_c)^a}{w_p L_p^a} - b\gamma \left[ \frac{w_c^2 (w_p + L_p)^a}{4w_p L_p^a \tan \beta} - \left( \frac{w_c^3}{24w_p L_p \tan \beta} \right)^a \right], \quad (1)$$

where  $P$  is the pillar average stress, MPa;  $w_p$ ,  $L_p$  and  $w_c$  are pillar width, pillar length and mining width respectively, m;  $\gamma$  is unit weight of overburden, N/m<sup>3</sup>;  $H$  is the mining depth, m;  $\beta$  is the abutment angle, °;  $a$  and  $b$  are coefficients.

**Table 1.** Well-known formulas in pillar average stress calculation for partial extraction mines [13,16,26].

Type	Formula Name	a	b	fi	Application Condition & Parameter Instruction
TAT	TAT [13,16,26]	2D 0 3D 1	0 0	-	The TAT method can be used for stress calculation of production pillars when the roof is intact, and mine size is large.
PAT	King (1970) [13,26]	2D 0 3D 1	1 1	31°	1. The PAT method (King, Wilson, Choi & McCain, Mark and Poulsen) can be used for stress calculation of pillars near caving roof, barrier pillars in room-and-pillar mining, strip pillar and longwall pillar. 2. 2D is for long strip pillars; 3D for small rectangular pillars. 3. If $w_c > 2H \tan \beta$ , $w_c = 2H \tan \beta$ in stress calculation; 4. $\beta$ was mostly summarized from longwall mining.
	Wilson (1970) [13,26]	2D 0 3D 1	1 1	16.7°	
	Choi & McCain (1980) [13]	2D 0 3D 1	1 1	18°	
	Mark (1987) [13]	2D 0 3D 1	1 1	21°	
	Poulsen (2010) [16]	2D 0 3D 1	1 1	$\tan^{-1}(0.27 - 10^{-4}H)$	

Table 2 shows the pillar stress calculation methods of longwall mining, which may also be helpful to the pillar strength calculation for underground strip pillar mining. Most formulae in Table 1 only focus on the stress calculation in pillars and do not combine the pillars and the overburden strata, while many formulae in Table 2 consider the properties of the overburden. Qian et al. [23] observed that the in-situ data collected in the field indicated that an intact strata or uniformly fractured strata may form part of geotechnical structures (e.g., the strata behave like arch, beam) and share the overburden weight, and proposed the key strata theory and constructed masonry beam models for roof stability analysis for longwall mining. They suggested that a key, strong strata would carry the weight of the above overburden while the strata below it will no longer carry the load, implying that the existence of the key strata may affect the stress distribution on the pillars, however, the role of key strata in room-and-pillar mining or underground strip pillar mining is still not very clearly studied.

**Table 2.** Well-known formulas in longwall pillar stress calculation [13,19–22,27,28].

Formula Name	Formula & Parameter Instruction
Salamon (1964) [21,27]	$P_T(x) = \frac{\gamma Hx}{\sqrt{x^2 - \frac{L^2}{4}}}$ Pillar stress at location $x$ can be calculated; the origin of $x$ is located at the center of longwall panel. $\gamma$ for unit weight of overburden, $N/m^3$ ; $H$ for the mining depth, $m$ ; $L$ for panel length, $m$ .
Mark (1987) [13]	$P_A(w_t) = P_A \left[ 1 - \left( \frac{5.13\sqrt{H-w_t}}{5.13\sqrt{H}} \right)^3 \right]$ The abutment load on pillar group is calculated (Figure 4); $P_A$ for abutment load; $H$ for the mining depth, $m$ ; $w_t$ for width of pillar group.
Majdi (1988) [22,28]	$P_A = \gamma H \left[ (0.08h^{0.55} + 0.7) \left( 0.002 \frac{E_p L}{E_o} \right)^{0.4} + 1 \right]$ $P_A(x) = \frac{\gamma HL}{2} \sqrt{\frac{2E_p}{E_o \lambda_H h}} e^{-x \sqrt{\frac{2E_p}{E_o \lambda_H h}}}$ $\gamma$ for unit weight of overburden, $N/m^3$ ; $H$ for the mining depth, $m$ ; $h$ for pillar height, $m$ ; $E_p$ and $E_o$ for elastic modulus of coal seam and overburden respectively, $GPa$ ; $L$ for panel length, $m$ .
Heasley (2000) [19,20]	$P_A(x) = \frac{\gamma HL}{2} \sqrt{\frac{2E_p}{E_o \lambda_H h}} e^{-x \sqrt{\frac{2E_p}{E_o \lambda_H h}}}$ Pillar stress at location $x$ can be calculated; the origin of $x$ is located at the center of longwall panel. $\gamma$ for unit weight of overburden, $N/m^3$ ; $H$ for the mining depth, $m$ ; $L$ for panel length, $m$ ; $E_p$ and $E_o$ for elastic modulus of coal seam and overburden respectively, $GPa$ ; $\lambda_H$ is the laminated constant; $h$ for pillar height, $m$ ; $v$ for Poisson’s ratio of overburden; $r_p$ for width of yield zone of pillar.
A.K. Singh et al. (2011) [21]	$P(max) = 0.025H + 8.646 \times 10^{-4} H I_c^{0.5}$ $IR = 0.16H + 9.63 \times 10^{-3} I_c; I_c = \frac{\sigma_c l_c^2 h_{os}}{3}$ $P(max)$ for ultimate vertical stress of coal pillar, $MPa$ ; $H$ for the mining depth ( $H < 200$ ), $m$ ; $\sigma_c$ for UCS of caved roof, $MPa$ ; $l_c^2$ for length of roof sample core, $cm$ ; $h_{os}$ for thickness of strong roof bed, $m$ ; $n = 1.2$ if RQD of rock $\geq 80\%$ , or $n = 1$ ; $IR$ is the influence range of abutment stress, $m$ .
Rezaei et al. (2015) [22]	$P_A(x) = \gamma \left( H - H_d \sqrt{\frac{H_d^2}{H_d^2 + x^2}} \right); H_d = \frac{\gamma^2 h H \left( \frac{h^2}{3} + H^2 + Hh \right) (E_o + \frac{E_p v_o}{E_1})}{(1-v) E_o \sigma_c^2}$ Pillar stress at location $x$ can be calculated; the origin of $x$ is located at the edge of longwall panel; $\gamma$ for unit weight of overburden, $N/m^3$ ; $H$ for the mining depth, $m$ ; $H_d$ for height of “dressed zone” (similar to height of pressure arch), $m$ ; $h$ for pillar height, $m$ ; $k$ for bulk factor of roof; $v$ for Poisson’s ratio of overburden; $\sigma_c$ for UCS of caved roof, $MPa$ .

The other limitations of current methods include: (a) most literature assumed a horizontal ground surface and horizontal seams and seldom includes the effects of varied terrain. It was found that the

topography above the mines can affect the mine stability: the valley topography may contribute to abnormal horizontal stress in the mine roof, such abnormal stress may lead to pillar or roof failures beneath the valley bottom [29–32]; (b) The abutment angle is a constant for load calculation, but the angle in fact varies during the mining process, and the mine size effects are neglected; also, the abutment angle summarized from longwall mining may not be suitable for partial extraction with pillars.

### 2.1.2. Coal Pillar Strength

The coal strength is believed to have a “size-and-shape effect”—the strength will decrease with an increase in coal pillar size or a decrease in the height-to-width ratio—but there exists a critical size beyond which the strength of a coal pillar will not decrease [33]. Linear or power functions of the pillar width–height ratio were adopted to calculate pillar strength [34]. Except for several special cases, the pillar strength formulae in general take the following form:

$$S_p = K \left( A + B \frac{w_p^C}{h^D} \right), \quad (2)$$

where  $S_p$  is pillar strength;  $K$  is coal strength;  $w_p$  is pillar width, m;  $h$  is pillar height, m;  $A$ ,  $B$ ,  $C$  and  $D$  are empirical parameters.

Table 3 summarizes parameters of Equation (2) and Table 4 summarizes other formulae with a different form. Hustrulid [33] proposed the formulae to transfer laboratory-scale strength into in-situ strength:

$$\sigma_m = \frac{\sigma_c}{\sqrt{D_p/d}} D_p \leq 0.914 \text{ m}, \quad (3)$$

$$\sigma_m = \frac{\sigma_c}{\sqrt{0.914/d}} D_p > 0.914 \text{ m}, \quad (4)$$

where  $\sigma_m$  is the in-situ strength of coal cube with size of  $D_p$  and  $\sigma_c$  is the strength of cube coal specimen with size of  $d$ .

**Table 3.** Parameters of Equation (2) [13,26,34–48].

	Formula Name	$K$	$A$	$B$	$C$	$D$	$w_p/h$
Linear	Bunting (1911) [26,34,38] Van Heerden (1974) [34,39] Sorenson (1978) [34,40]	$S_1 = 7 \text{ MPa}$	0.7	0.3	1	1	0.5–3.4
	Obert-Duvall/Wang (1967) [13,26,36,37,41] Bieniawski (1975) [13,26,34–37,42,43]	$\sigma_m$ $\sigma_B$	0.778 0.64	0.222 0.36	1 1	1 1	1–8 <5
	Zern (1928) [26,34,37,44]	$S_1$	0	1	0.5	0.5	-
	Stear (1954) [34,45,46] Holland-Gaddy (1962) [13,26,34,47]	$S_1$ or $\sigma_c/\sqrt{d}$	0	1	0.5	1	2–8
Power	Greenwald (1941) [34,37,46] Salamon and Munro (1967) [26,34–37,46] Hedley & Grant (1972) [34,36,48]	$0.67\sigma_c$ $7.176 \text{ MPa}$ $\sigma_B$	0 0 0	1 1 1	0.5 0.46 0.5	5/6 0.66 0.75	<5
	Merwe and Mathey Squat pillar (2013) [35]	6.61 MPa 5.47 MPa	0 0	1 1	0.5 0.8	0.7 1	<12

**Parameter Explanation**

$S_1$  for in-situ coal stress, MPa;  $\sigma_m$  for in-situ UCS (uniaxial compressive strength) of a cubic specimen with a critical size, m;  $\sigma_B$  for UCS of a 30 cm long cubic specimen;  $d$  for specimen size, cm;  $\sigma_c$  for strength of coal cube ( $d = 2.5 \text{ cm}$ ).

**Table 4.** Other pillar strength formulas [20,34–37,49–52].

Formula Name	Formula & Parameter Instruction	$w_p/h$
Logie and Matheson (1982) [37,49]	$S_p = \sigma_B(0.64 + 0.34\frac{w_p}{h})^{1.4}$ $\sigma_B$ for UCS of a 30 cm long cubic specimen; $w_p$ for pillar width, m; $h$ for pillar height, m.	>5
Maleki (1992) [35,50]	$S_p = 32(1 - e^{-0.339\frac{w_p}{h}})$ MPa (confinement) $S_p = 26(1 - e^{-0.264\frac{w_p}{h}})$ Mpa (structural) $w_p$ for pillar width, m; $h$ for pillar height, m.	10–15
Sheorey (1992) [35,37,51]	$S_p = 0.27\sigma_c h^{-0.36} + (\frac{H}{250} + 1)(\frac{w_p}{h} - 1)$ $\sigma_c$ for strength of coal cube (specimen size $d = 2.5$ cm); $h$ for pillar height, m; $H$ for mining depth, m; $w_p$ for pillar width, m.	<6.7
Mark-Bieniawski (1997) [20,37,52]	$S_p = S_1[0.64 + (0.54\frac{w_p}{h} - 0.18\frac{w_p^2}{hL_p})]$ $S_1$ for in-situ coal stress, MPa; $h$ for pillar height, m; $w_p$ for pillar width, m; $L_p$ for pillar length, m.	
Salamon Squat Pillar (1982) [35,53]	$S_p = S_1 \frac{R_0^{0.5933}}{V_p^{0.0667}} \left\{ \frac{0.5933}{\epsilon} \left[ \left( \frac{R_p}{R_0} \right)^\epsilon - 1 \right] + 1 \right\}$ $S_1$ for in-situ coal stress, MPa; $R_0$ for critical width-height ratio of pillar and $R_0 = 5$ ; $\epsilon$ for rate of strength increase and $\epsilon = 2.5$ ; $V_p$ for pillar volume; $R_p$ for width-height ratio of pillar.	>5
Lunder (1997) (rock) [34]	$S_p = 0.44\sigma_u(0.68 + 0.52k_{1p})$ $k_{1p} = \tan \left[ \cos^{-1} \left( \frac{1 - c_{pav}}{1 + c_{pav}} \right) \right]$ ; $c_{pav} = 0.46 \left[ \log \left( \frac{w_p}{h} + 0.7 \right) \right]^{\frac{1.4}{w_p/h}}$ $w_p$ for pillar width, m; $h$ for pillar height, m; $\sigma_u$ for UCS of intact sample of pillar material (5 cm), MPa.	

The applications of these formulae are limited due to their empirical nature: The size and shape of pillars are not the only essential factors affecting the pillar strength, coal structures such as cleat, joint, porosity or other micro-flaws can also affect pillar strength. However, they are not well considered in these equations. By analyzing 4000 individual tests resulting from over 60 seams, Mark [54] found that there exists a poor correlation between sample strength and size effect and concluded that only the “blocky” coal has an obvious “size effect”. The explanation of “size effect” is that the mechanical parameters of rock can be affected by randomly-distributed micro structures, thus the mechanical properties of rock will show randomness when the rock size varies. The oversimplification of these correlations may lead to inaccurate results.

The REV (representative elementary volume) of rock material is proposed to determine the critical volume that represents the strength of intact rocks. If the specimen size exceeds the REV, the randomly-distributed micro-structures can be assumed to be uniformly distributed and the mechanical properties of the rock mass can be defined by homogenized-statistical rock properties. Many researchers have attempted to characterize the REV properties of rocks including macro-mechanical properties, micro-structures and hydraulic properties of rock mass [55–64].

A limitation of the classical method is the lack of inclusion of time-dependent effects of pillar degradation: Weathering effects, especially of water intrusion, have a long-term impact on pillar strength. The effect of water may be activated after mining activities have stopped, as the maintenance of the mine system ceases. Many room-and-pillar voids were found to collapse after 1–3 years of abandonment in China. The situation may be more severe if there is an aquifer that floods the abandoned mine shafts.

### 2.1.3. Pillar Yielding Area

To address the issue of underestimating pillar strength, the concept of “yielding pillar” is proposed, which assumes that the pillar consists of a “confined core” that supports most of the loads and a surrounding plastic zone that provides constraint to the core. The plastic zone loses its capacity partially or totally, thus, to ensure stability, the width of the pillar should exceed the yielding plastic zone to make sure the “core” exists [13,18].

The strength of the pillar core is calculated based on limit equilibrium theory as:

$$S_p = \frac{2C \cos \varphi}{1 - \sin \varphi} + \frac{1 + \sin \varphi}{1 - \sin \varphi} \lambda \gamma H = UCS + \frac{1 + \sin \varphi}{1 - \sin \varphi} \lambda \gamma H, \quad (5)$$

where  $C$  is the coal cohesion, MPa;  $\varphi$  is the coal internal friction angle, °;  $\lambda$  is the coefficient of horizontal stress at yield/elastic plate;  $UCS$  is the uniaxial compressive strength of coal, MPa.

The formulae of the plastic zone extent  $r_p$  are in Table 5. To ensure the capacity of the pillar, pillar width is also suggested to satisfy [23]:

$$w_p > 2(r_p + h), \quad (6)$$

**Table 5.** Yield depth calculation formula [18,26,65,66].

Formula Name	Formula	Parameter Explanation
Wilson (1972) [26]	$r_p = 4.92 \times 10^{-3} h H$	$h$ for pillar height, m; $H$ for mining depth, m
Wilson (1983) [18]	Yield only occur in coal seam $r_p = \frac{h}{F} \ln\left(\frac{\gamma H}{p}\right)$ Yield occur in roof, coal seam and floor $r_p = \frac{h}{2} \left[ \left( \frac{\gamma H}{p} \right)^{\frac{1}{\sqrt{\eta}-1}} - 1 \right]$	$h$ for pillar height, m; $H$ for mining depth, m; $F = \frac{\eta-1}{\sqrt{\eta}} + \left( \frac{\eta-1}{\sqrt{\eta}} \right)^2 \tan^{-1} \sqrt{\eta}$ ; $\eta = \frac{1+\sin\varphi}{1-\sin\varphi}$ ; $p$ for restraint stress at pillar rib, MPa; $\gamma$ for unit weight of overburden, N/m <sup>3</sup>
Bai (1983) [65]	$r_p = \frac{w_c}{2} \left( \frac{1}{\sqrt{1 - \left( \frac{F_k \gamma H}{\sigma_{yi} \tau \gamma H} \right)}} - 1 \right)$	$\gamma$ for unit weight of overburden, N/m <sup>3</sup> ; $H$ for mining depth, m; $w_c$ for mining width, m; $\sigma_{yi}$ for coal yield stress, MPa; $F_k = (0.595 + 0.875 \frac{w_c}{w_c + w_p})(0.9831 + 0.0106N)$ , $N$ for strip pillar number;
Wu (1995) [66]	$r_p = \frac{d\lambda h}{2 \tan \varphi} \ln\left(1 + \frac{\sigma_{ul}}{\sigma_c} \tan \varphi\right) + \frac{d}{2} h \tan \varphi$	$h$ for pillar height, m; $d = 1.5-3$ for stress disturbance factor (damages on pillar rib); $\sigma_{ul}$ for coal ultimate strength, MPa; $\sigma_c$ for pillar average compressive strength, MPa; $\lambda$ for coefficient of horizontal stress at yield/elastic plate.

The yielding pillar design method is widely applied in longwall and strip pillar designs. It provides a better strength estimate for wider pillars in deep seams where non-uniform stress distribution occurs. However, the lack of analysis of coal structures and material degradation make it not suitable for long-term stability assessments.

## 2.2. Numerical Simulation Methods

Numerical simulation methods include continuum-based (finite difference method, finite element method, boundary element method, etc.) and non-continuum-based methods (discrete element method, rigid block-joint element method, etc.). Through numerical simulation, the mining conditions can be easily evaluated, and it is less costly to conduct systematic analysis, which is sometimes not possible for in-situ investigation or physical simulation. The behavior of a single pillar [67] and a roof-pillar-floor system [68,69] have been studied using numerical simulation. More complicated mining conditions and dynamic processes, such as jointed overburden strata [70], multi-seam mining [71], and domino-like collapse disaster of room-and-pillar mines [72], can also be investigated. Numerical simulation methods have been an important tool in mine design and mine behavior analysis [73–78].

However, the accuracy of simulation results is questionable as the results depend on the model assumptions and the accuracy of the input parameters. The rock mass usually contains macro- and micro-discontinuities that significantly affect the mechanical properties of rock mass, but it is hard to acquire these realistic material properties to conduct a reliable numerical simulation. The shortcomings also come from the oversimplification of both 2D and 3D models in representing the complex mine site situation, the uncertainty of input parameters, and the neglect of complete stress–strain relations for individual rock materials and the theoretical limitations that are inherent in simulation methods [78]. Although there exist arguments regarding the accuracy of simulation results, there is no better replaceable method to perform systematic, full-size analysis of mines. Numerical simulations are effective to analyze the effect of multiple factors on mine stability. As numerical simulations can also be used to study the hydromechanical behaviors of a mine [79–82], and the underground mine cavities may be infused with water, numerical simulation may be a powerful tool to study the mechanisms of the long-term instability of partial extraction mines. When utilizing numerical simulation methods, it is necessary to select proper models and input parameters according to the research purpose.

The theoretical analysis, laboratory test and in-situ investigation can be combined to ensure the validity of numerical simulation results.

### 2.3. Physical Simulation Methods

Based on similitude theory and dimensional analysis [83,84], similar material simulation is widely used in physical modeling in the coal industry [85–90]. With similar material simulation, an in-situ large-scale mine can shrink down to a laboratory-scale model, and the behavior of the small models can be similar to the behavior of the mine prototype. The dimensional analysis can be used to derive the similarity criterion [84]. Both the stability of mines and dynamic phenomena such as strata movement, crack distribution, crack propagation and cave-in, can be analyzed with physical models, which are difficult for numerical modeling or in-situ investigation [85–90]. Furthermore, physical simulation method provides a reliable reference in checking the validity of numerical outcomes.

However, there still exist some shortages of similar material simulations. First, it is hard to simulate weak discontinuities, such as joints in rock mass. It is also sometimes difficult to construct reliable models or specimens containing fissures that are desired (e.g., the simulation of internal fissures in rock) in actual simulations. This shortage reduces the applicability of similar material simulations in the analysis of fractured rock masses or joint-affected rocks. Second, the study of the material components and their proportions is still limited. It is hard to simulate the plastic behavior of rock mass. Finally, the model properties are affected by humidity, temperature and time [88,89], which means the applicability of similar material simulations in the long-term behavior analysis of mining pillars may be restricted.

### 2.4. Other Methods

As the properties of coal can vary significantly at different geologies, and the critical safety factor for a stable pillar is different in different coal seams, reliability-based models have been used in underground mine stability assessments; for example, Sun [91] developed a reliability-based PESH (point estimate and safety margin) method for the stability assessment of mine entry; Wattimena et al. [92] proposed a probability-based stability prediction model with logistic regression. Fuzzy theories were used to analyze the occurrence of sinkholes [93] and to predict coal pillar size for room-and-pillar mines [94]; Hu et al. [95] built a Bayes discriminant analysis-based model to classify the risk level of waste mines; and neural networks [96] and support vector machines [97] have also been introduced for mine stability assessments.

However, reliability-based stability assessment methods are still based on safety factors with the same limitations of the classical pillar design theories; other methods such as logistic regression are classification methods, they are dependent on the historical data and rationality of input parameters.

## 3. Discussion of Influence Factors on Mine Stability

Pillar strength can be influenced by several factors described in the following:

### 3.1. Influence of Coal and Mine Structures

Structural features such as cleat, joint, slips and “non-coal” mineral partings are discontinuities in coal pillars. York [98] attempted to use the rock mass classification method and Ramamurthy method [99] to estimate the effect of joints on pillar strength in relation to joint frequency, orientation and joint conditions. Esterhuizen [100] found that discontinuities in coal can significantly reduce pillar strength if the width-to-height ratio is small. Biswas [101] found that some non-coal mineral partings can reduce the strength of coal pillars in the presence of water. Finally, Hill [102] further found that the effect of discontinuities will decrease if the width-to-height ratio of a pillar increases.

### 3.2. Influence of Weathering

Rock weathering can result from water, bacteria and temperature differentials. The effects of water originate from hydraulic pressurization and hydro-chemical reactions. The weathering effects can degrade the mechanical properties of coal pillars and reduce the pillar size. Salamon [103], Van der Merwe [104] and Esterhuizen et al. [105] found that the pillar scales down with time, and defined it as progressive pillar failure. Such scaling down of pillars is induced by rib spalling, which is further driven by water, stress, crack expansion, etc. Van der Merwe [106] assumed that pillar size is a function of time and that a pillar fails when the safety factor  $<0.3$ , and proposed a pillar life index to predict the minimum life span of a coal pillar:

$$d_p = w_p - [0.0742h^{0.265}H^{0.437}(w_p + w_c)^{0.813}], \quad (7)$$

$$R_p = 0.015h^{3.7}, \quad (8)$$

$$\text{Life index} = d_p/R_p, \quad (9)$$

where  $d_p$  is the peeling amount allowed;  $w_p$  is the pillar width;  $w_c$  is the mining width;  $h$  is the pillar height;  $H$  is the mining depth;  $R_p$  is the rate of scaling.

Similar research was also conducted by Salmi et al. [107]. However, such pillar scaling (or pillar peeling) is not limitless. The coal fragments can peel from the pillar rib and accumulate around a pillar during the pillar scaling progress [103,108,109], and stable coal debris piles may finally form around the scaled coal pillars, providing horizontal confinement to the pillar rib and preventing the pillars from further scaling down [108,109].

Biswas [101] has found that the mineral partings of coal pillars are more sensitive to water than coal. The degradation of coal pillars is in fact the weathering effect on partings in a coal pillar, and the strength reduction of coal and partings at different weathering times,  $t$  (year) can be defined as:

$$\rho_{coal} = \frac{\sigma_{coal-t}}{\sigma_{coal-i}} = 100(1.01 - e^{-3.5d_r}) - 0.13t, \quad (10)$$

$$\rho_{part} = \frac{\sigma_{part-t}}{\sigma_{part-i}} = 100(1.01 - e^{-0.5d_r}) - 0.45t, \quad (11)$$

where  $d_r$  is the depth into the pillar from rib;  $\sigma_{coal-i}$  and  $\sigma_{part-i}$  are the initial intact strength of coal and parting,  $\sigma_{coal-t}$  and  $\sigma_{part-t}$  are the strength of coal and parting at the time of  $t$  and location of  $d_r$ .  $\rho_{coal}$  and  $\rho_{part}$  are the reduction coefficients at position  $d_r$  and time  $t$ . The area where the reduction coefficient is below 60% is believed to be the weathered zone.

Recent research also showed that the mechanical properties of rock material (e.g., rock strength, rock stiffness, the fracture toughness of rock, the elastic modulus of rock, etc.) may degrade due to water [110–120]. Poulsen et al. [121] suggested that the strength reduction of saturated coal pillars can be estimated by the average strength reduction of all the lithological components of coal.

### 3.3. Influence of Spontaneous Combustion of Coal

An underground coal fire is a critical issue for almost all coal producing countries: Kuenzer et al. [122,123] and Song et al. [124] summarized the status of coal fires worldwide and in China, respectively. Coal spontaneous combustion is associated with pyrite oxidation, bacteria effects, oxidation of the phenolic group and the coupled effect of oxygen and coal. Whether an underground coal fire will occur depends on the spontaneous combustion susceptibility of the coal and the conditions surrounding the mines. The susceptibility to coal spontaneous combustion is affected by coal rank and coal components, mining depth, coal seam thickness, humidity, temperature and air circulation [124–130].

Wang et al. [130] studied the fracture distribution of longwall mining and believed that the air for combustion comes into the mine shafts through fissures from fractured overburden. The atmospheric pressure change has notable effects on the longwall mine temperature field [131], which are dictated by the porosity of coal pillars and oxygen flow in the pillar. Considering gas flow, Qi et al. [125] estimated the combustion zone width in the shafts.

Kuenzer et al. [122,123] summarized the effects of coal seam fires on landforms into surface fracture, surface subsidence (e.g., sinkholes, slides) and bedrock changes. Coal spontaneous combustion is a critical origin of the production of greenhouse and toxic gases [132] and an important aspect of land reutilization and sustainable development [133], burning and post-burning coal seam management and the combustion control of longwall-mining [125,130,131,134]. Although some pillars in abandoned mines were reported to suffer spontaneous combustion in China, studies of the combustion possibility of abandoned mines for partial extraction are relatively limited. It is believed that the fissures on ground surfaces, the leakage of the mine shafts besides the working face and residual coal in the abandoned mines can cause spontaneous combustion [130,134,135]. Therefore, abandoned mine stability may also interact with the combustion of residual coal pillars for some mines.

#### 3.4. Influence of Roof and Floor Properties

The stability of room-and-pillar mine shafts depends on the properties of the roof, pillar and floor system, a non-destructive stiff pillar may punch into roof and floor, causing mine instability [54,72,136–138]. Dynamic hazards such as coal bumps depend on the properties of the whole mining system, and most bumps appear to occur in strong roof and floor scenarios [138]. Collapse-quakes can be critical, with energy originated from the release of the elastic energy accumulated in the strata [138]. The extent of the plastic zone and the influence of mining-induced stress are also associated with properties of the roof and floor [18,54]. The mining depth and the roof stability dictate if the sinkholes can appear on the ground surface (the roof failure may develop at the ground surface if the mining depth is shallow, leading to sinkholes on the ground surface), and beam theories can be used to analyze the roof stability.

#### 3.5. Influence of Pillar Shape and Other Factors

The pillar shape can dictate its failure modes [54,139]. Hill [102] summarized a pillar database in South Africa and Australia and found that most collapsed pillars had a low width-to-height ratio. Slender pillars with a width-to-height ratio less than three or four may lead to a sudden, massive collapse. For intermediate pillars with a width-to-height ratio between four and eight, the failure form appears to be “squeeze”, and for squat pillars with a width-to-height ratio exceeding 10, the failure may start from the roof or floor [54]. A logical explanation is that when the coal pillar is slender, the load condition is more likely to be in a uniaxial state than a triaxial state due to the lack of lateral stress to pillar core. Besides the fact that the pillar strength and the pillar failure model are affected by the pillar shape, the pillar scaling progress is also affected by the pillar shape [108].

Other factors that may affect the stability of mine voids include ground stress, temperature and artificial disturbance. The strength of rock and the probability of rock burst will increase with high ground stress [138,140]. Ground stress and the properties of the material, such as cohesion and fracture toughness, are affected by changes in temperature [140–142]. The temperature variation of most room-and-pillar mines is induced by geothermal temperature, which usually depends on mining depth, indicating that the temperature effect is negligible for such mine cases.

## 4. Discussion of Improving Stability Assessment Methods

The assessment of mine failures is typically difficult and it is hard to establish the causation and outcome relationships. Hence, reliance on strong rationalization is essential. Figure 5 summarizes the mechanism of mine void support failure and a rationale algorithm to establish mine shaft instability causation. To detect mine failure, classical rock classification methods can be used: For example, the Hoek–Brown failure criterion has parameters concerning the type and integrity of rock. Other methods

such as the RQD, and Q-classification methods are widely accepted in rock classification and can be used for the initial assessment of rock mass stability. The joint roughness coefficient (JRC) can be used to calculate the shearing strength of joints in coal pillar design [98]. Salmi et al. suggested that rock classification methods should be considered when utilizing the mechanical rock properties, such as Young's modulus, Poisson's ratio, UCS [107]. For example, he suggested that the coal seam strength can be estimated as:

$$K = 0.5 \left( \frac{RMR - 15}{85} \right) \sigma_{ci}, \quad (12)$$

where  $K$  is the coal strength;  $\sigma_{ci}$  is the UCS of a specimen (specimen diameter is 54 mm; ratio of specimen length to diameter is 2 to 2.5);  $RMR$  is the rock mass rating that related to rock classification [107].

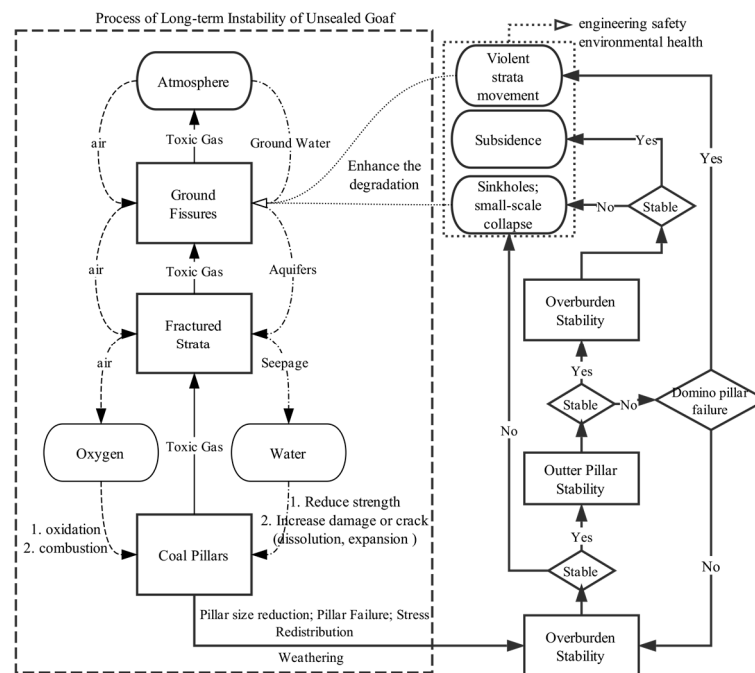


**Figure 5.** Schematic of mine instability: dashed line for air flow; solid line for toxic gas; dash-dot line for water flow.

Both damage mechanics and fracture mechanics connect the discontinuities in material-to-pillar failures and are closer to realistic rock behaviors. The progressive pillar scaling down [103,107–109] and strength degradation [121] are associated with discontinuity expansion and damage evolution, such damage accumulations will result in pillar rib spalling, a reduction of effective pillar size, etc. [101,105,107–109,143], leading to the long-term instability of pillars. The utilizations of these two methods may be helpful to establish time-dependent failure criteria and damage evolution models. The analysis of pillar creep behavior is another method to study time-dependent pillar stability. The pillar stress may increase with time due to progressive pillar failure, the pillar stress should never exceed the creep pillar strength to keep the long-term stability [103,107–109]. The pillar stability assessment should not only depend on the safety factors and yielding pillar design methods but should include these methods to correlate rock discontinuities and long-term pillar behavior to pillar support capacity.

However, existing fracture-based mechanics do not comprehensively describe the evolution of the failure history. For example, the expansion of discontinuous planes induced by dissolution results in the volume expansion of partings in pillars and may lead to a low-stress failure. Studies of fracture mechanics and damage mechanics must be coupled with field measurements using non-destructive

testing (NDT) technologies, such as acoustic emission [144–146] and CT (Computed Tomography) scans [147,148], which can be used to investigate failure during continuous loading.

As stated previously, the mechanical properties of small rock specimens show randomness, due to random effects of micro-structures, hence, it may not be representative to evaluate the mine stability. REV methods can be used so that the scale level of the rock that can be treated as a continuum material can be established.

The weathering effects, especially the effect of water, is believed to be the key element dictating the long-term stability of abandoned mines. The dissolution of non-coal partings can be treated as crack expansion, with its length calculated with the dissolved parting volume and parting thickness. The crack expansion rate has relevance to the dissolution rate of the material. Time-dependent material degradation can be estimated by the ionic concentration and dissolution rate, and the probable failure time can be estimated by analyzing the status of the coal pillar.

Due to imperfect knowledge of the rock mass and coupling effects of many factors, it is still hard to evaluate long-term pillar behavior. Thus, the empirical methods, such as Van der Merwe's [104,106] prediction method of pillar life, are still needed for site application, especially when the problems urgently need to be solved [14].

The stability of both underground engineering structures (e.g., tunnel, mineral pillar, roof and floor) and ground surface should be verified to ensure that they meet the requirement of mining-waste land reutilization. However, the study of the relationship between ground surface displacement and mechanical failure mechanisms of underground structures is insufficient, making it hard to evaluate the effect of underground instability on ground surface movement. To link the underground instability with ground surface displacement, the entire mine structure should be treated as a system and the effect of the overburden structures, including overburden key strata [130], rock bursts [149] and roof stability [150] should not be ignored.

The detection of precursors of mine-subsidence-induced micro seismicity are of great interest to the research community: Acoustic emission techniques [144–146], infrared thermography [151], laser scanning [152] and the SAR (synthetic aperture radar) techniques [153–158] have been utilized to study the precursors of rock failure. SAR techniques, in particular, may have the most potential to assess the performance of partial extraction mines, because they can provide accurate, cumulative regional displacements of ground surface. If the failure precursors exist, the laws of these precursors for room-and-pillar mines can be developed, which is useful for long-term stability monitoring and locating unknown old mines or illegal mines.

Finally, the spontaneous combustion of coal should be considered. Since coal can absorb oxygen when the temperature exceeds  $-80\text{ }^{\circ}\text{C}$ , the heat will be released, and the temperature will increase during oxygen absorption [159]. If the temperature exceeds  $50\text{ }^{\circ}\text{C}$ , the chemical absorption of oxygen will become significant, and unstable hydrocarbon–oxygen complexes (work within the range of  $50\text{--}120\text{ }^{\circ}\text{C}$ ) will form, and the chemical activities of coal will be enhanced [159]. If the heat accumulation rate is larger than the heat emanation rate, the temperature and the chemical reaction between coal and oxygen will increase drastically beyond the ignition point of the coal and combustion will occur. Hence, to evaluate the possibility of spontaneous combustion, the oxidation properties of coal (including the oxidation effects on combustion and strength degradation), the air circulation condition and the temperature field of the abandoned mines should be investigated first. Whether the combustion of residual pillars is a long-term threat to the safety of land use should be clear.

## 5. Conclusions and Outlook

The stability of the abandoned mine is an engineering problem critical for land reutilization and environmental protection. It is one of the important issues that the mining cities must face when designed using sustainable development principles. The key role of abandoned mine stability assessment is to classify the future danger levels of these ground voids, so that the treatment of the abandoned mine voids can be managed, and the subsidence lands can be fully used according to

land stability. Also, the laws and precursors of post-mining hazards need to be investigated to locate unknown mine voids. This paper summarized current state-of-the-art of design theories of partial extraction mines and factors affecting mine stability, which may also provide a scientific basis for forensic subsidence evaluation. For the forensic subsidence evaluation of partial extraction mines, an understanding of subsidence mechanisms and mine design theories is important. Since more complicated subsidence problems (e.g., whether the pillar collapses, the effects of pillar failure on the ground surface, the range of secondary subsidence induced by pillar failure, the causation of the subsidence, etc.) are related to the mine design theories.

The shortcomings of traditional subsidence theories and pillar design theories have prevented their applications for evaluating the long-term mine stability of partial extraction, making it hard to provide scientific support for land reutilization. Thus, more research is needed to advance assessment methodologies to identify the factors affecting the long-term stability of partial extraction mines. It is believed that the structural planes in pillars and water are the key factors in the long-term stability of abandoned mines. The factors summarized should be considered or be introduced to the existing stability evaluation methods.

To provide a better evaluation, a systematic mine void stability assessment method should be established, which should include initial stability evaluation, long-term stability evaluation, potential failure time, features of potential collapse disasters, effects of failure hazards on ground structure health, methods to relieve or eliminate potential dangers, damage responsibility confirmation, compensation evaluation and maintenance direction.

The stability evaluation of partial extraction mines is a complex problem and involves a large number of factors. The stability evaluation of partial extraction mines can be separated into two parts: one is the stability evaluation of underground pillars, and the other is the stability evaluation of the roof. The stability evaluation of underground pillars can further be separated into initial stability evaluation and long-term stability evaluation. The initial stability evaluation can be used for pillar design, and the stability evaluation of coal pillars during the coal-producing process. The purpose of the initial pillar design is to ensure mine safety during production, and post-mining subsidence and its effects on ground structures can be excluded. The primary considerations for initial stability evaluations include pillar strength, the width–height ratio of the pillar, and the stress on pillars. The pillar strength can be acquired by laboratory experiments, in-situ tests or back-analysis of historical pillar cases. Current mine design theories have provided significant support for initial stability evaluations. While the purpose of long-term stability evaluations is to prevent further ground subsidence and protect ground structures and the environment. Besides the pillar strength, the width–height ratio and the pillar stress, long-term stability evaluations should also consider the time-dependent strength degradation and size reduction of coal pillars (pillar peel behavior) that is induced by multiple factors, such as weathering and the intrusion of underground water, so that the long-term stability of the pillar can be known, and the potential pillar failure time can be estimated. Recent research shows that fractured coal fragments can peel from the pillar and accumulate by pillars during time-dependent pillar size reduction, and may finally form a stable fragment pile that helps to restrict continuous pillar size reduction [108], thus, time-dependent pillar size reduction may not be limitless for some partial extraction mines, and these mines may still have the ability to remain stable long-term, although their stability has degraded due to multiple factors. However, the current literature on long-term stability evaluations is relatively limited. Further efforts are needed to study the time-dependent strength of peeled pillars, the effects of peeled coal fragments on pillar stability, the ultimate peeling depth into the pillars, etc. By the same token, the stability evaluation method of mine rooves above rooms should be improved. The time-dependent strength degradation of overburden and its effect on the occurrence of sinkholes should be further studied, which may include the effects of overburden properties (e.g., overburden structure, lithology) and mining depth on roof stability, the time-dependent strength degradation of rooves induced by weathering or water, the effect of roof instability on the occurrence of sinkholes, etc. Finally, post-collapse disasters (e.g., mining-induced earthquake, ground fissures, etc.) should also be studied

and summarized when analyzing mine stability, as they may be helpful to subsidence prediction and forensic subsidence evaluation. Interdisciplinary knowledge and cooperation are needed to overcome difficulties in technological advancements, such as new sensors and sensing techniques.

**Acknowledgments:** Financial support is provided by (1) the National Nature Science Fund of China (41604005), and (2) the State Key Laboratory of Geohazard Prevention and Geo-Environment Protection (Chengdu University of Technology) (SKLGP2016K008).

**Author Contributions:** Ka-Zhong Deng, Shen-En Chen, Peng Wang and Hong-Dong Fan all provided the topics, ideas and technical instructions of the study; Yang Yu wrote the paper; Shen-En Chen provided language support and revised the paper.

**Conflicts of Interest:** The authors declare no conflict of interest.

## References

1. Bureau of Land Management of U.S. Available online: <http://www.abandonedmines.gov> (accessed on 5 October 2017).
2. Bian, Z.; Miao, X.; Lei, S.; Chen, S.; Wang, W.; Struthers, S. The challenges of reusing mining and mineral-processing wastes. *Science* **2012**, *337*, 702–703. [[CrossRef](#)] [[PubMed](#)]
3. Ministry of Land and Resources of China. 2008. Available online: [http://www.mlr.gov.cn/xwdt/jrxw/200805/t20080507\\_102527.htm](http://www.mlr.gov.cn/xwdt/jrxw/200805/t20080507_102527.htm) (accessed on 5 October 2017). (In Chinese)
4. Shaanxi Earthquake Information Network. Available online: <http://www.eqsn.gov.cn/> (accessed on 7 December 2017).
5. Yin, Y.; Ren, H. Turning “Waste” into Wealth—The Recovery Ratio of Coal Resource Is Doubled Due to the Improvement of Pillar Recovery Technique. 2007. Available online: [http://jjckb.xinhuanet.com/cjxw/2007-08/14/content\\_61914.htm](http://jjckb.xinhuanet.com/cjxw/2007-08/14/content_61914.htm) (accessed on 7 December 2017). (In Chinese)
6. Li, C.; Ren, J.; Wen, H.; Xu, W.; Gong, T.; Wang, M. Impact of coal mining subsidence on loss of soil moisture and nutrients and ecological environment. *J. Anhui Agric. Sci.* **2013**, *40*, 4343–4344. (In Chinese)
7. Wang, J.; Du, H.; Wang, S. Analysis of damage process and mechanism for plant community and soil properties at northern Shenmu subsidence mining area. *J. China Coal Soc.* **2017**, *42*, 17–25. (In Chinese)
8. He, W.; Xiang, M.; Liu, H.; Li, Y.; Peng, J. Ground subsidence and its environment problems in Yushenfu mining area. *Coal Geol. Explor.* **2016**, *44*, 131–135. (In Chinese)
9. Zhang, F.; Zhao, H.; Song, Y.; Chen, L. The effect of coal-mining subsidence on water environment in the Shenfu-Dongsheng mining area. *ACTA Geosci. Sin.* **2007**, *28*, 521–527. (In Chinese)
10. Kivinen, S. Sustainable post-mining land use: Are closed metal mines abandoned or re-used space? *Sustainability* **2017**, *9*, 1705. [[CrossRef](#)]
11. He, G.Q.; Yang, L.; Ling, G.D.; Jia, F.C.; Hong, D. *Mine Subsidence Science*; China University of Mining and Technology Press: Xuzhou, China, 1994. (In Chinese)
12. Bell, F.G.; Genske, D.D. The influence of subsidence attributable to coal mining on the environment, development and restoration: Some examples from Western Europe and South Africa. *Environ. Eng. Geosci.* **2001**, *7*, 81–99. [[CrossRef](#)]
13. Mark, C. Analysis of Longwall Pillar Stability. Ph.D. Thesis, Pennsylvania State University, University Park, PA, USA, 1987.
14. Mark, C. Science of empirical design in mining ground control. *Int. J. Min. Sci. Technol.* **2016**, *26*, 461–470. [[CrossRef](#)]
15. Hauquin, T.; Deck, O.; Gunzburge, Y. Average vertical stress on irregular elastic pillars estimated by a function of the relative extraction ratio. *Int. J. Rock. Mech. Min.* **2016**, *83*, 122–134. [[CrossRef](#)]
16. Poulsen, B.A. Coal pillar load calculation by pressure arch theory and near field extraction ratio. *Int. J. Rock Mech. Min.* **2010**, *47*, 1158–1165. [[CrossRef](#)]
17. Yu, Y.X.; Huang, R.B.; Wang, B.Q. Analysis on limit equilibrium zone of coal pillar in mining roadway based on mechanical model of elastic foundation beam. *J. Eng. Mech.* **2016**, *142*. Available online: [https://doi.org/10.1061/\(ASCE\)EM.1943-7889.0001032](https://doi.org/10.1061/(ASCE)EM.1943-7889.0001032) (accessed on 4 January 2018). [[CrossRef](#)]
18. Wilson, A.H. The stability of underground workings in the soft rocks of the coal measures. *Int. J. Min. Eng.* **1983**, *1*, 91–187. [[CrossRef](#)]

19. Heasley, K.A. The forgotten denominator, pillar loading. In Proceedings of the 4th North American Rock Mechanics Symposium, Seattle, WA, USA, 31 July–3 August 2000.
20. Heasley, K.A. Some thoughts on calibrating LaModel. In Proceedings of the 27th International Conference on Ground Control in Mining, Morgantown, WV, USA, 29–31 July 2008.
21. Singh, A.K.; Singh, R.; Maiti, J.; Kumar, R.; Mandal, P.K. Assessment of mining induced stress development over coal pillars during depillaring. *Int. J. Rock Mech. Min.* **2011**, *48*, 805–818. [[CrossRef](#)]
22. Rezaei, M.; Hossaini, M.F.; Majdi, A. Determination of longwall mining-induced stress using the strain energy method. *Rock Mech. Rock Eng.* **2015**, *48*, 1–13. [[CrossRef](#)]
23. Qian, M.G.; Shi, P.W.; Xu, J.L. *Mine Pressure and Strata Control*; China University of Mining and Technology Press: Xuzhou, China, 2010. (In Chinese)
24. Hatzor, Y.H.; Benary, R. The stability of a laminated Voussoir beam: Back analysis of a historic roof collapse using DDA. *Int. J. Rock Mech. Min. Sci.* **1988**, *35*, 165–181. [[CrossRef](#)]
25. Zhao, T.; Liu, C.; Yetilmezsoy, K.; Zhang, B.; Zhang, S. Fractural structure of thick hard roof stratum using long beam theory and numerical modeling. *Environ. Earth Sci.* **2017**, *76*, 751. [[CrossRef](#)]
26. Wu, L.; Wang, J.; Guo, Z. *Foundation for Coal Pillar Design and Monitoring*; China University of Mining and Technology Press: Xuzhou, China, 2000. (In Chinese)
27. Salamon, M.D.G. Elastic analysis of displacements and stress induced by the mining of seam or reef deposits, Part II. *J. S. Afr. Inst. Min. Metall.* **1964**, *64*, 197–218.
28. Majdi, A. The Stability of Face Access Tunnel in the Deep Soft Rocks of Coal Mining. Ph.D. Thesis, McGill University, Montreal, QC, Canada, 1988.
29. Griffith, W.A.; Becker, J.; Cione, K.; Miller, T.; Pan, E. 3D topographic stress perturbations and implications for ground control in underground coal mines. *Int. J. Rock Mech. Min.* **2014**, *70*, 59–68. [[CrossRef](#)]
30. Molinda, G.M.; Heasley, K.A.; Oyler, D.C.; Jones, J.R. *Effects of Horizontal Stress Related to Stream Valleys on the Stability of Coal Mine Openings*; US Department of the Interior, Bureau of Mines: Washington, DC, USA, 1992.
31. Mark, C.; Mucho, T.P.; Dolinar, D. Horizontal stress and longwall headgate ground control. *Min. Eng.* **1998**, *50*, 61–68.
32. Xu, W.Y.; Zhang, J.C.; Wang, W.; Wang, R.B. Investigation into in situ stress fields in the asymmetric V-Shaped river valley at the Wudongde Dam site, Southwest China. *Bull. Eng. Geol. Environ.* **2014**, *73*, 465–477. [[CrossRef](#)]
33. Hustrulid, W.A. A review of coal pillar strength formulas. *Rock Mech.* **1976**, *8*, 115–145. [[CrossRef](#)]
34. Lunder, P.J. Hard rock pillar strength estimation—An applied empirical approach. Master's Thesis, University of British Columbia, Vancouver, BC, Canada, 1994.
35. Mathey, M.; Van der Merwe, J.N. Critique of the South African squat coal pillar strength formula. *J. S. Afr. Inst. Min. Metall.* **2016**, *116*, 291–299. [[CrossRef](#)]
36. Rastiello, G.; Federico, F.; Screpanti, S. New soft rock pillar strength formula derived through parametric FEA using a critical state plasticity model. *Rock Mech. Rock Eng.* **2015**, *48*, 2077–2091. [[CrossRef](#)]
37. Verma, A.K. A comparative study of various empirical methods to estimate the factor of safety of coal pillars. *Am. J. Min. Metall.* **2014**, *2*, 17–22.
38. Bunting, D. Chamber-pillars in deep anthracite mines. *Trans. Am. Inst. Min. Eng.* **1911**, *42*, 739–748.
39. Van Heerden, W.L. *In-Situ Determination of Complete Stress-Strain Characteristics of 1.4 m Square Specimens with Width to Height Ratios up to 3.4*; Council for Scientific and Industrial Research: Pretoria, South Africa, 1974.
40. Sorenson, W.K.; Pariseau, W.G. Statistical analysis of laboratory compressive strength and Young's modulus data for the design of production pillars in coal mines. In Proceedings of the 19th U.S. Symposia on Rock Mechanics, Reno, NV, USA, 1–3 May 1978.
41. Overt, L.; Duvall, W.I. *Rock Mechanics and the Design of Structures in Rock*; John Wiley & Sons: New York, NY, USA, 1967.
42. Bieniawski, Z.T. The effect of specimen size on the compressive strength of coal. *Int. J. Rock Mech. Min. Sci.* **1968**, *5*, 325–335. [[CrossRef](#)]
43. Bieniawski, Z.T.; van Heerden, W.L. The significance of in situ tests on large rock specimen. *Int. J. Rock Mech. Min. Sci.* **1975**, *12*, 101–113. [[CrossRef](#)]
44. Zern, E.N. *Coal Miner's Pocketbook*; McGraw Hill: New York, NY, USA, 1928.
45. Steart, F.A. Strength and stability of pillars in coal mines. *J. Chem. Metall. Min. Soc. S. Afr.* **1954**, *54*, 309–325.

46. Salamon, M.D.G.; Munro, A.H. A study of the strength of coal pillars. *J. S. Afr. Inst. Min. Metall.* **1967**, *68*, 55–67.
47. Holland, C.T. The strength of coal in mine pillars. In Proceedings of the 6th U.S. Symposia on Rock Mechanics, Rolla, MO, USA, 28–30 October 1964.
48. Hedley, D.G.F.; Grant, F. Stope and pillar design for the Elliot Lake uranium mines. *Can. Inst. Min. Metall. Bull.* **1972**, *65*, 37–44.
49. Logie, C.V.; Matheson, G.M. A critical review of the current state-of-the-art design of mine pillar. In Proceedings of the 1st International Conference on Stability in Underground Mining, Vancouver, BC, Canada, 16–18 August 1982.
50. Maleki, H. In situ pillar strength and failure mechanisms for US coal seams. In Proceedings of the Workshop on Coal Pillar Mechanics and Design, Santa Fe, NM, USA, 7 June 1992.
51. Sheorey, P.R. Pillar strength considering in situ stresses. In Proceedings of the Workshop on Coal Pillar Mechanics and Design, Santa Fe, NM, USA, 7 June 1992.
52. Galvin, J.M. *Ground Engineering—Principles and Practices for Underground Coal Mining*; Springer International Publishing: Cham, Switzerland, 2016.
53. Salamon, M.D.G.; Wagner, H. Practical experience in the design of coal pillars. In Proceedings of the 21st International Conference of Safety in Mines Research Institutes, Sydney, Australia, 21–25 October 1985.
54. Mark, C. The evolution of intelligent coal pillar design: 1981–2006. In Proceedings of the 25th International Conference on Ground Control in Mining, Morgantown, WV, USA, 1–3 August 2006.
55. Zhu, Q.Z.; Shao, J.F. A refined micromechanical damage–friction model with strength prediction for rock-like materials under compression. *Int. J. Solids Struct.* **2015**, *60–61*, 75–83. [[CrossRef](#)]
56. Yang, J.P.; Chen, W.Z.; Yang, D.S.; Yuan, J.Q. Numerical determination of strength and deformability of fractured rock mass by FEM modeling. *Comput. Geotech.* **2015**, *64*, 20–31.
57. Wang, M.; Kulatilake, P.H.S.W. Understanding of hydraulic properties from configurations of stochastically distributed fracture networks. *Hydrol. Process.* **2008**, *22*, 1125–1135. [[CrossRef](#)]
58. Zhang, T.T.; Yan, E.C.; Hu, X.M.; Cao, Y.B. Fractal description of rock mass structure representative elementary volume. *Adv. Mater. Res.* **2012**, *594–597*, 439–445. [[CrossRef](#)]
59. Khani, A.; Baghbanan, A.; Hashemolhosseini, H. Numerical investigation of the effect of fracture intensity on deformability and REV of fractured rock masses. *Int. J. Rock Mech. Min.* **2013**, *63*, 104–112. [[CrossRef](#)]
60. Xia, L.; Zheng, Y.; Yu, Q. Estimation of the REV size for blockiness of fractured rock masses. *Comput. Geotech.* **2016**, *76*, 83–92. [[CrossRef](#)]
61. Esmaili, K.; Hadjigeorgiou, J.; Grenon, M. Estimating geometrical and mechanical REV based on synthetic rock mass models at Brunswick mine. *Int. J. Rock Mech. Min.* **2010**, *47*, 915–926. [[CrossRef](#)]
62. Wu, Q.; Kulatilake, P.H.S.W. REV and its properties on fracture system and mechanical properties, and an orthotropic constitutive model for a jointed rock mass in a dam site in china. *Comput. Geotech.* **2012**, *43*, 124–142. [[CrossRef](#)]
63. Riyadh, A. Change in microstructure parameters of porous media over representative elementary volume for porosity. *Part. Sci. Technol.* **2012**, *30*, 1–16.
64. Li, J.H.; Zhang, L.M. Geometric parameters and REV of a crack network in soil. *Comput. Geotech.* **2010**, *37*, 466–475. [[CrossRef](#)]
65. Bai, M.; Liu, T. Study on pillar size and mining width for partial mining. *J. China Coal Soc.* **1983**, *4*, 19–26. (In Chinese)
66. Wu, L.; Wang, J. Calculation of width of yield zone of coal pillar and analysis of influence factors. *J. China Coal Soc.* **1995**, *20*, 625–631. (In Chinese)
67. Jaiswal, A.; Shrivastva, B.K. Numerical simulation of coal pillar strength. *Int. J. Rock Mech. Min.* **2009**, *46*, 779–788. [[CrossRef](#)]
68. Shabanimashcool, M.; Li, C.C. A numerical study of stress changes in barrier pillars and a border area in a longwall coal mine. *Int. J. Coal Geol.* **2013**, *106*, 39–47. [[CrossRef](#)]
69. Kostecki, T.; Spearing, A.J.S. Influence of backfill on coal pillar strength and floor bearing capacity in weak floor conditions in the Illinois Basin. *Int. J. Rock Mech. Min.* **2015**, *76*, 55–67. [[CrossRef](#)]
70. He, L.; Zhang, Q.B. Numerical investigation of arching mechanism to underground excavation in jointed rock mass. *Tunn. Undergr. Space Technol.* **2015**, *50*, 54–67. [[CrossRef](#)]

71. Wei, X.Q.; Bai, H.B.; Rong, H.R.; Jiao, Y.; Zhang, B.Y. Research on mining fracture of overburden in close distance multi-seam. *Procedia Earth Planet. Sci.* **2011**, *2*, 20–27. [[CrossRef](#)]
72. Li, C.; Xu, J.; Wang, Z.; Qin, S. Domino instability effect of surrounding rock-coal pillars in a room-and-pillar gob. *Int. J. Min. Sci. Technol.* **2013**, *23*, 913–918. [[CrossRef](#)]
73. Gao, W.; Ge, M. Stability of a coal pillar for strip mining based on an elastic-plastic analysis. *Int. J. Rock Mech. Min. Sci.* **2016**, *87*, 23–28. [[CrossRef](#)]
74. Li, G.; Cao, S.; Li, Y.; Zhang, Z. Load bearing and deformation characteristics of granular spoils under unconfined compressive loading for coal mine backfill. *Adv. Mater. Sci. Eng.* **2016**, *2016*, 8530574. [[CrossRef](#)]
75. Ghabraie, B.; Ghabraie, K.; Ren, G.; Smith, J.V. Numerical modelling of multistage caving processes: Insights from multi-seam longwall mining-induced subsidence. *Int. J. Numer. Anal. Methods Geomech.* **2017**, *41*, 959–975. [[CrossRef](#)]
76. Zhang, J.; Shen, B. Coal mining under aquifers in China: A case study. *Int. J. Rock Mech. Min. Sci.* **2004**, *41*, 629–639. [[CrossRef](#)]
77. Fama, M.E.D.; Trueman, R.; Craig, M.S. Two- and three-dimensional elasto-plastic analysis for coal pillar design and its application to highwall mining. *Int. J. Rock Mech. Min. Sci. Geomech. Abstr.* **1995**, *32*, 215–225. [[CrossRef](#)]
78. Peng, S.S. Topical areas of research needs in ground control—a state of the art review on coal mine ground control. *Int. J. Min. Sci. Technol.* **2015**, *25*, 1–6. [[CrossRef](#)]
79. Bidgoli, M.N.; Jing, L. Water pressure effects on strength and deformability of fractured rocks under low confining pressures. *Rock Mech. Rock Eng.* **2015**, *48*, 971–985. [[CrossRef](#)]
80. Mortimer, L.; Aydin, A.; Simmons, C.T.; Love, A.J. Is in situ stress important to groundwater flow in shallow fractured rock aquifers? *J. Hydrol.* **2011**, *399*, 185–200. [[CrossRef](#)]
81. Benmebarek, N.; Benmebarek, S.; Kastner, R. Numerical studies of seepage failure of sand within a cofferdam. *Comput. Geotech.* **2005**, *32*, 264–273. [[CrossRef](#)]
82. Ma, D.; Miao, X.; Bai, H.; Huang, J.; Pu, H.; Wu, Y.; Zhang, G.; Li, J. Effect of mining on shear sidewall groundwater inrush hazard caused by seepage instability of the penetrated Karst collapse pillar. *Nat. Hazards* **2016**, *82*, 73–93. [[CrossRef](#)]
83. Kline, S.J. *Similitude and Approximation Theory*; McGraw-Hill Book Company: New York, NY, USA, 1965.
84. Butterfield, R. Dimensional analysis for geotechnical engineering. *Geotechnique* **1999**, *49*, 357–366. [[CrossRef](#)]
85. Wu, K.; Cheng, G.; Zhou, D. Experimental research on dynamic movement in strata overlying coal mines using similar material modeling. *Arab. J. Geosci.* **2015**, *8*, 6521–6534. [[CrossRef](#)]
86. Chen, S.; Wang, H.; Zhang, J.; Xing, H.; Wang, H. Low-strength similar materials for backfill mining: Insight from experiments on components and influence mechanism. *Geotech. Test. J.* **2015**, *38*, 929–935. [[CrossRef](#)]
87. Zhou, S.; Wu, K.; Zhou, D.; Li, L.; Xu, Y. Experimental study on displacement field of strata overlying goaf with sloping coal seam. *Geotech. Geol. Eng.* **2016**, *34*, 1–10. [[CrossRef](#)]
88. Zha, J.; Li, H.; Guo, G.; Wang, J. Influence of temperature and humidity on similar material and its control measures. *Environ. Earth Sci.* **2017**, *76*, 740. [[CrossRef](#)]
89. Li, H.; Guo, G.; Zha, J. Study on time-varying characteristics of similar material model strength and the regulation measures. *Environ. Earth Sci.* **2017**, *76*, 518. [[CrossRef](#)]
90. Ghabraie, B.; Ren, G.; Zhang, X.; Smith, J. Physical modelling of subsidence from sequential extraction of partially overlapping longwall panels and study of substrata movement characteristics. *Int. J. Coal Geol.* **2015**, *140*, 71–83. [[CrossRef](#)]
91. Sun, Z.V. Reliability-Based Method for Stability of Mine Entry Design and Evaluation. Ph.D. Thesis, West Virginia University, Morgantown, WV, USA, 2000.
92. Wattimena, R.K.; Kramadibrata, S.; Sidi, I.D.; Azizi, M.A. Developing coal pillar stability chart using logistic regression. *Int. J. Rock Mech. Min.* **2013**, *58*, 55–60. [[CrossRef](#)]
93. Deb, D.; Choi, S.O. Analysis of sinkhole occurrences over abandoned mines using Fuzzy reasoning: A case study. *Geotech. Geol. Eng.* **2006**, *24*, 1243–1258. [[CrossRef](#)]
94. Ghasemi, E.; Ataei, M.; Shahriar, K. An intelligent approach to predict pillar sizing in designing room and pillar coal mines. *Int. J. Rock Mech. Min.* **2014**, *65*, 86–95. [[CrossRef](#)]
95. Hu, Y.X.; Li, X.B. Bayes discriminant analysis method to identify risky of complicated goaf in mines and its application. *Trans. Nonferrous Metals Soc. China* **2012**, *22*, 425–431. [[CrossRef](#)]

96. Tang, S.L.; Tang, H.; Guo, H. Stability evaluation of empty mine goaf based on BP neural network. *J. Xian Univ. Sci. Technol.* **2012**, *32*, 234–238. (In Chinese)
97. Zhou, J.; Li, X.; Mitri, H.S.; Wang, S.; Wei, W. Identification of large-scale goaf instability in underground mine using particle swarm optimization and support vector machine. *Int. J. Min. Sc. Technol.* **2013**, *23*, 701–707. [[CrossRef](#)]
98. York, G.; Canbulat, I.; Jack, B.W. Coal Pillar Design Procedures. 2000. Available online: <http://researchspace.csir.co.za/dspace/handle/10204/1419> (accessed on 5 October 2017).
99. Ramamurthy, T.; Rao, G.V.; Singh, J. A strength criterion for anisotropic rocks. In Proceedings of the 5th Australia-New Zealand Conference on Geomechanics, Sydney, Australia, 22–26 August 1988.
100. Esterhuizen, G.S. Investigations into the effect of discontinuities on the strength of coal pillars. *J. S. Afr. Inst. Min. Metall.* **1997**, *97*, 57–61.
101. Biswas, K. Study of Weathering Actions on Partings and Its Effects on Long Term Stability of Coal Pillar. Ph.D. Thesis, West Virginia University, Morgantown, WV, USA, 1997.
102. Hill, D. Coal pillar design criteria for surface protection. In Proceedings of the Coal Operators' Conference, Wollongong, Australia, 26–28 April 2005; pp. 31–38.
103. Salamon, M.D.G.; Ozbay, M.U.; Madden, B.J. Life and design of bord-and-pillar workings affected by pillar scaling. *J. S. Afr. Inst. Min. Metall.* **1998**, *98*, 135–145.
104. Van der Merwe, J.N. Predicting coal pillar life in South Africa. *J. S. Afr. Inst. Min. Metall.* **2003**, *5*, 293–301.
105. Esterhuizen, G.S.; Dolinar, D.R.; Ellenberger, J.L. Pillar strength in underground stone mines in the United States. *Int. J. Rock. Mech. Min.* **2011**, *48*, 42–50. [[CrossRef](#)]
106. Van der Merwe, J.N. Revised strength factor for coal in the Vaal Basin. *J. S. Afr. Inst. Min. Metall.* **1993**, *93*, 71–77.
107. Salmi, E.F.; Nazem, M.; Karakus, M. The effect of rock mass gradual deterioration on the mechanism of post-mining subsidence over shallow abandoned coal mines. *Int. J. Rock Mech. Min.* **2017**, *91*, 59–71. [[CrossRef](#)]
108. Yu, Y.; Chen, S.E.; Deng, K.Z.; Fan, H.D. Long-term stability evaluation and pillar design criterion for room-and-pillar mines. *Energies* **2017**, *10*, 1644. [[CrossRef](#)]
109. Peng, S.S. *Ground Control Failures: A Pictorial View of Case Studies*; West Virginia University Press: Morgantown, WV, USA, 2007.
110. Nara, Y.; Morimoto, K.; Hiroyoshi, N.; Yoneda, T.; Kaneko, K.; Benson, P.M. Influence of relative humidity on fracture toughness of rock: Implications for subcritical crack growth. *Int. J. Solids Struct.* **2012**, *49*, 2471–2481. [[CrossRef](#)]
111. Wong, L.N.Y.; Maruvanchery, V.; Liu, G. Water effects on rock strength and stiffness degradation. *Acta Geotech.* **2016**, *11*, 713–737. [[CrossRef](#)]
112. Shi, X.; Cai, W.; Meng, Y.; Li, G.; Wen, K.; Zhang, Y. Weakening laws of rock uniaxial compressive strength with consideration of water content and rock porosity. *Arab. J. Geosci.* **2016**, *9*, 369. [[CrossRef](#)]
113. Vásárhelyi, B.; Ván, P. Influence of water content on the strength of rock. *Eng. Geol.* **2006**, *84*, 70–74. [[CrossRef](#)]
114. Yilmaz, I. Influence of water content on the strength and deformability of gypsum. *Int. J. Rock Mech. Min.* **2010**, *47*, 342–347. [[CrossRef](#)]
115. Vergara, M.R.; Triantafyllidis, T. Influence of water content on the mechanical properties of an argillaceous swelling rock. *Rock Mech. Rock Eng.* **2016**, *49*, 2555–2568. [[CrossRef](#)]
116. Khamrat, S.; Archeeploha, S.; Fuenkajorn, K. Pore pressure effects on strength and elasticity of ornamental stones. *Scienceasia* **2016**, *42*, 121–135. [[CrossRef](#)]
117. Masoumi, H.; Horne, J.; Timms, W. Establishing empirical relationships for the effects of water content on the mechanical behavior of Gosford sandstone. *Rock Mech. Rock Eng.* **2017**, *50*, 2235–2242. [[CrossRef](#)]
118. Pellet, F.L.; Keshavarz, M.; Boulon, M. Influence of humidity conditions on shear strength of clay rock discontinuities. *Eng. Geol.* **2013**, *157*, 33–38. [[CrossRef](#)]
119. Zhou, Z.; Cai, X.; Cao, W.; Li, X.; Xiong, C. Influence of water content on mechanical properties of rock in both saturation and drying processes. *Rock Mech. Rock Eng.* **2016**, *49*, 3009–3025. [[CrossRef](#)]
120. Liu, L.; Xu, W.Y.; Wang, H.L.; Wang, R.B.; Wang, W. Experimental studies on hydro-mechanical properties of metamorphic rock under hydraulic pressures. *Eur. J. Environ. Civ. Eng.* **2016**, *20*, 45–59. [[CrossRef](#)]

121. Poulsen, B.A.; Shen, B.; Williams, D.J.; Huddleston-Holmes, C.; Erarslan, N.; Qin, J. Strength reduction on saturation of coal and coal measures rocks with implications for coal pillar strength. *Int. J. Rock Mech. Min.* **2014**, *71*, 41–52. [[CrossRef](#)]
122. Kuenzer, C.; Stracher, G.B. Geomorphology of coal seam fires. *Geomorphology* **2012**, *138*, 209–222. [[CrossRef](#)]
123. Kuenzer, C.; Zhang, J.; Tetzlaff, A.; Dijk, P.V.; Voigt, S.; Mehl, H.; Wagner, W. Uncontrolled coal fires and their environmental impacts: Investigating two arid mining regions in north-central China. *Appl. Geogr.* **2007**, *27*, 42–62. [[CrossRef](#)]
124. Song, Z.; Kuenzer, C. Coal fires in China over the last decade: A comprehensive review. *Int. J. Coal Geol.* **2014**, *133*, 72–99. [[CrossRef](#)]
125. Qi, L.M.; Chen, X.X. Theory analysis on spontaneous combustion zone width in the middle of goaf. *Procedia Earth Planet. Sci.* **2009**, *1*, 322–327.
126. Ray, S.K.; Panigrahi, D.C.; Udayabhanu, G.; Saxena, V.K. Assessment of spontaneous heating susceptibility of Indian coals—A new approach. *Energy Sources Part A* **2016**, *38*, 59–68. [[CrossRef](#)]
127. Kim, J.; Lee, Y.; Ryu, C.; Park, H.Y.; Lim, H. Low-temperature reactivity of coals for evaluation of spontaneous combustion propensity. *Korean J. Chem. Eng.* **2015**, *32*, 1297–1304. [[CrossRef](#)]
128. Tang, Y.; Xue, S. Laboratory study on the spontaneous combustion propensity of lignite undergone heating treatment at low temperature in inert and low-oxygen environments. *Energy Fuel* **2015**, *29*, 4683–4689. [[CrossRef](#)]
129. Huang, X.H. Research on Fire Control Technology of Residual Pillar Mining with Spontaneous Combustion in Mine. Ph.D. Thesis, China University of Mining and Technology (Beijing), Beijing, China, 2015. (In Chinese)
130. Wang, S.; Li, X.; Wang, D. Void fraction distribution in overburden disturbed by longwall mining of coal. *Environ. Earth Sci.* **2016**, *75*, 1–17. [[CrossRef](#)]
131. Wang, G.; Luo, H.Z.; Liang, Y.T.; Wang, J.R. Temperature field simulation of gob influenced by atmospheric pressure. *J. Cent. South Univ.* **2015**, *22*, 4366–4371. [[CrossRef](#)]
132. Wang, H.; Chen, C. Experimental study on greenhouse gas emissions caused by spontaneous coal combustion. *Energy Fuel* **2015**, *29*, 5213–5221. [[CrossRef](#)]
133. Voigt, S.; Tetzlaff, A.; Zhang, J.; Künzer, C.; Zhukov, B.; Strunz, G.; Oertel, D.; Roth, A.; Dijk, P.V.; Mehl, H. Integrating satellite remote sensing techniques for detection and analysis of uncontrolled coal seam fires in North China. *Int. J. Coal Geol.* **2004**, *59*, 121–136. [[CrossRef](#)]
134. Xia, T.; Zhou, F.; Liu, J.; Kang, J.; Gao, F. A fully coupled hydro-thermo-mechanical model for the spontaneous combustion of underground coal seams. *Fuel* **2014**, *125*, 106–115. [[CrossRef](#)]
135. Lu, Y.; Qin, B. Identification and control of spontaneous combustion of coal pillars: A case study in the Qianyingzi mine, China. *Nat. Hazards* **2015**, *75*, 2683–2697. [[CrossRef](#)]
136. Qin, S.; Jiao, J.J.; Tang, C.A.; Li, Z. Instability leading to coal bumps and nonlinear evolutionary mechanisms for a coal-pillar-and-roof system. *Int. J. Solids Struct.* **2006**, *43*, 7407–7423. [[CrossRef](#)]
137. Ma, H.; Wang, J.; Wang, Y. Study on mechanics and domino effect of large-scale goaf cave-in. *Saf. Sci.* **2012**, *50*, 689–694. [[CrossRef](#)]
138. Qi, Q.X.; Dou, L.M. *Coal Bump Theories and Technologies*; China University of Mining and Technology Press: Xuzhou, China, 2008. (In Chinese)
139. Poulsen, B.A.; Shen, B. Subsidence risk assessment of decommissioned bord-and-pillar collieries. *Int. J. Rock Mech. Min.* **2013**, *60*, 312–320. [[CrossRef](#)]
140. Zhou, Q.C. Study on the Mechanical Property of a Sandstone under Geothermal-Mechanical and Hydraulic-Mechanical Coupling. Ph.D. Thesis, Chinese Academy of Science, Beijing, China, 2006. (In Chinese)
141. Funatsu, T.; Kuruppu, M.; Matsui, K. Effects of temperature and confining pressure on mixed-mode (I–II) and mode II fracture toughness of Kimachi sandstone. *Int. J. Rock Mech. Min.* **2014**, *67*, 1–8. [[CrossRef](#)]
142. Nara, Y.; Yamanaka, H.; Oe, Y.; Kaneko, K. Influence of temperature and water on subcritical crack growth parameters and long-term strength for igneous rocks. *Geophys. J. Int.* **2013**, *193*, 47–60. [[CrossRef](#)]
143. Castellanza, R.; Gerolymatou, E.; Nova, R. An attempt to predict the failure time of abandoned mine pillars. *Rock Mech. Rock Eng.* **2008**, *41*, 377–401. [[CrossRef](#)]
144. Peyras, L.; Rivard, P.; Breul, P.; Millet, A.; Ballivy, G. Characterization of rock discontinuity openings using acoustic wave amplitude—Application to a metamorphic rock mass. *Eng. Geol.* **2015**, *193*, 402–411. [[CrossRef](#)]

145. Moradian, Z.; Einstein, H.H.; Ballivy, G. Detection of cracking levels in brittle rocks by parametric analysis of the acoustic emission signals. *Rock Mech. Rock Eng.* **2016**, *49*, 785–800. [[CrossRef](#)]
146. Wieser, C.; Käsling, H.; Raith, M.; Richter, R.; Moser, D.; Gemander, F.; Grosse, C.; Thuro, K. Acoustic emission technique to detect micro cracking during uniaxial compression of brittle rocks. *Eng. Geol. Soc. Territ.* **2015**, *6*, 465–468.
147. Yu, Q.; Yang, S.; Ranjith, P.G.; Zhu, W.; Yang, T. Numerical modeling of jointed rock under compressive loading using x-ray computerized tomography. *Rock Mech. Rock Eng.* **2016**, *49*, 877–891. [[CrossRef](#)]
148. Pini, R.; Madonna, C. Moving across scales: A quantitative assessment of X-ray CT to measure the porosity of rocks. *J. Porous Mater.* **2016**, *23*, 325–338. [[CrossRef](#)]
149. Feng, X.; Wang, E.; Shen, R.; Wei, M.; Chen, Y.; Cao, X. The dynamic impact of rock burst induced by the fracture of the thick and hard key stratum. *Procedia Eng.* **2011**, *26*, 457–465.
150. Ju, J.; Xu, J.; Zhu, W. Longwall chock sudden closure incident below coal pillar of adjacent upper mined coal seam under shallow cover in the Shendong coalfield. *Int. J. Rock Mech. Min.* **2015**, *77*, 192–201. [[CrossRef](#)]
151. Gong, W.; Peng, Y.; He, M.; Wang, J. Thermal image and spectral characterization of roadway failure process in geologically 45° inclined rocks. *Tunn. Undergr. Space Technol.* **2015**, *49*, 156–173. [[CrossRef](#)]
152. Abellán, A.; Oppikofer, T.; Jaboyedoff, M.; Rosser, N.J.; Lim, M.; Lato, M.J. Terrestrial laser scanning of rock slope instabilities. *Earth Surf. Process. Landf.* **2014**, *39*, 80–97. [[CrossRef](#)]
153. Sousa, J.J.; Bastos, L. Multi-temporal SAR interferometry reveals acceleration of bridge sinking before collapse. *Nat. Hazards Earth Syst.* **2013**, *13*, 659–667. [[CrossRef](#)]
154. Lazecký, M.; Çomut, F.C.; Hlaváčová, I.; Gürboğa, S. Practical application of satellite-based SAR interferometry for the detection of landslide activity. *Procedia Earth Planet. Sci.* **2015**, *15*, 613–618. [[CrossRef](#)]
155. Li, Z.; Wang, J.; Li, L.; Wang, L.; Liang, R.Y. A case study integrating numerical simulation and GB-InSAR monitoring to analyze flexural toppling of an anti-dip slope in Fushun open pit. *Eng. Geol.* **2015**, *197*, 20–32. [[CrossRef](#)]
156. Huang, J.; Deng, K.; Fan, H.; Yan, S. An improved pixel-tracking method for monitoring mining subsidence. *Remote Sens. Lett.* **2016**, *7*, 731–740. [[CrossRef](#)]
157. Fan, H.; Gao, X.; Yang, J.; Deng, K.; Yu, Y. Monitoring mining subsidence using a combination of phase-stacking and offset-tracking methods. *Remote Sens.* **2015**, *7*, 9166–9183. [[CrossRef](#)]
158. Chen, B.; Deng, K.; Fan, H.; Yu, Y. Combining SAR interferometric phase and intensity information for monitoring of large gradient deformation in coal mining area. *Eur. J. Remote Sens.* **2015**, *48*, 701–717. [[CrossRef](#)]
159. Pone, J.D.N.; Hein, K.A.A.; Stracher, G.B.; Annegarn, H.J.; Finkleman, R.B.; Blake, D.R.; McCormack, J.K.; Schroeder, P. The spontaneous combustion of coal and its by-products in the Witbank and Sasolburg coalfields of South Africa. *Int. J. Coal Geol.* **2007**, *72*, 124–140. [[CrossRef](#)]

